Nucleic Acids Research, 1998, Vol. 26, No. 16 **3717–3723**

Interaction of structural modules in substrate binding by the ribozyme from *Bacillus subtilis* RNase P

Lindsay Odell[+], Victor Huang, Monika Jakacka and Tao Pan*

Department of Biochemistry and Molecular Biology, University of Chicago, Chicago, IL 60637, USA

Received May 4, 1998; Revised and Accepted June 29, 1998

ABSTRACT

The ribozyme from bacterial ribonuclease P recognizes two structural modules in a tRNA substrate: the T stem–loop and the acceptor stem. These two modules are connected through a helical linker. The T stem–loop binds at a surface confined in a folding domain away from the active site. Substrates for the *Bacillus subtilis* RNase P RNA were previously selected *in vitro* that are shown to bind comparably well or better than a tRNA substrate. Chemical modification of P RNA–substrate complexes with dimethylsulfate and kethoxal was performed to determine how the P RNA recognizes three *in vitro* selected substrates. All three substrates bind at the surface known to interact with the T stem–loop of tRNA. Similar to a tRNA, the secondary structure of these substrates contains a helix around the cleavage site and a hairpin loop at the corresponding position of the T stem–loop. Unlike a tRNA, these two structural modules are connected through a non-helical linker. The two structural modules in the tRNA and in the selected substrates bind to two different domains in P RNA. The properties of substrate recognition exhibited by this ribozyme may be exploited to isolate new ribozyme–substrate pairs with interactive structural modules.

INTRODUCTION

The RNA component from ribonuclease P is unique among natural ribozymes because of its ability to recognize pre-formed RNA structures. RNase P is a processing enzyme responsible for producing the mature 5′ end of all tRNAs *in vivo* (1,2). Bacterial RNase P is composed of a 330–420nt RNA (denoted P RNA) and a 13–15 kDa protein. Bacterial P RNA is an efficient ribozyme at high ionic strength. P RNA primarily recognizes the coaxially stacked helical structure composed of the acceptor stem and the T stem–loop of tRNA (summarized in 3 and 4). The specificity is conferred by the groove-like structure formed by the T stem–loop within the tRNA tertiary structure (5).

Novel RNA substrates for either the *Escherichia coli* M1 RNA and holoenzyme (6) or the *Bacillus subtilis* P RNA (7,8) have been obtained by *in vitro* selection. When the full-length *B.subtilis* P RNA was used (7), the selected substrates could be classified into four groups (representative substrates designated as #4, #8, #17 and #22). When a subdomain of the *B.subtilis* P RNA was used (8), a single substrate (designated as variant #1) was isolated. Variant #1 has the same sequence as substrate #8 and it contains a pseudoknot structure in place of the T stem–loop in tRNA. This pseudoknot interacts with a region of P RNA that plays no role in the binding of a tRNA substrate (8).

This paper examines how P RNA recognizes the three other *in vitro* selected substrates, #4, #17 and #22. Each selected substrate contains a short helix around the cleavage site and a hairpin loop resembling the T stem–loop of tRNA. These two structural modules are connected through a non-helical linker region. Chemical modification of the ribozyme and ribozyme-3′ product complexes identifies a binding surface in the P RNA that significantly overlaps with the binding surface of tRNA. These results suggest that P RNA recognizes two structural modules in the substrate. These substrates, in turn, bind to two structural modules in P RNA that are represented by its two folding domains (9,10).

MATERIALS AND METHODS

Preparation of RNA

The P RNA from *B.subtilis* and the selected substrates were obtained by *in vitro* transcription using T7 RNA polymerase (11). The plasmids containing templates for #4, #8 and #17 were cloned and isolated from the initial selection experiment (7). The oligonucleotide template for a minimal construct of #22 was made by automated DNA synthesis. The sequence, 5′-TGGTGCGAATTCTGAAGGGTGATTACCTTAGTTTTCGGTGCTATAGTGAGTCGTATTA (T7 promoter sequence underlined) encodes the 3′ 40 nt of #22 plus a 5′G to improve transcription. This minimal construct has identical cleavage efficiency as the full-length #22 (data not shown).

Chemical modification using dimethylsulfate (DMS) and kethoxal (KE)

The P RNA and the substrates were renatured separately by heating at 85–90°C for 2 min followed by incubation at 22°C for 3 min. $MgCl_2$ was added to P RNA to appropriate concentrations and the mixture was incubated at 50°C for 10 min. $MgCl_2$,

*To whom correspondence should be addressed. Tel: +1 773 702 4179; Fax: +1 773 702 0439; Email: taopan@midway.uchicago.edu

[+]Present address: BCMB Program, The Johns Hopkins University School of Medicine, Baltimore, MD 21205, USA

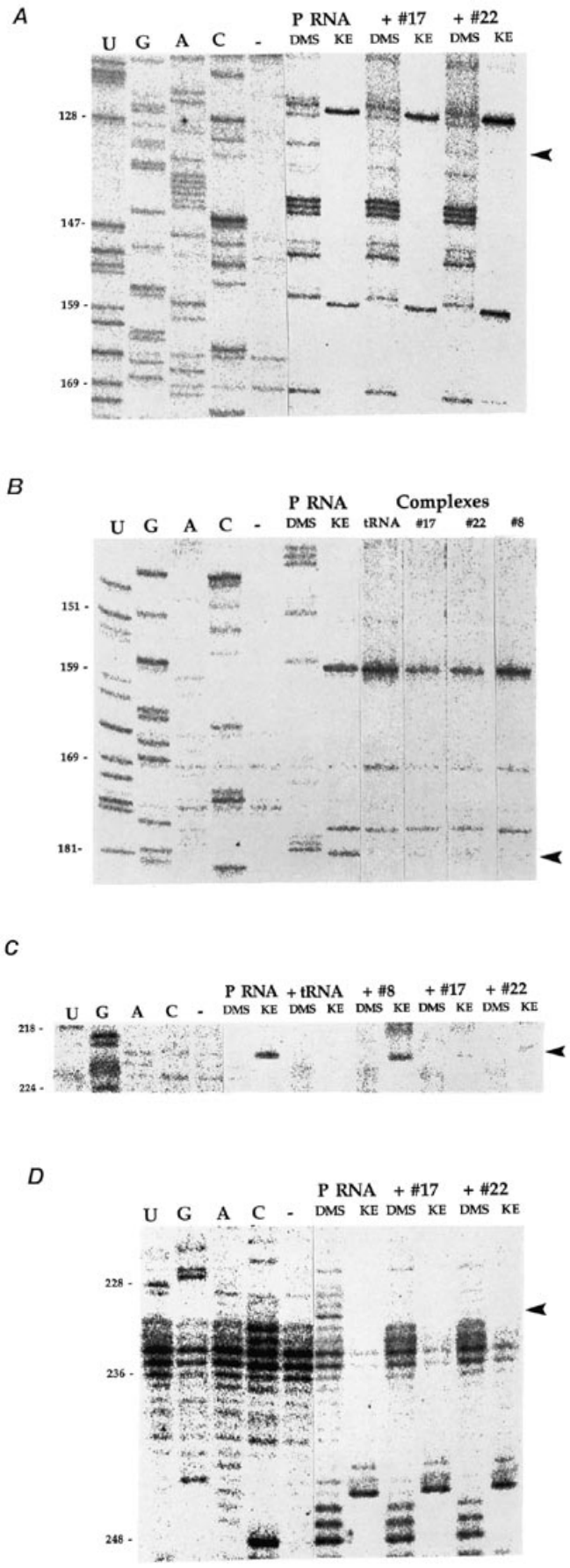

spermine or KCl were added to appropriate substrates followed by incubation at 37°C for 5 min. Each substrate was reacted with P RNA at 37°C for 15 min to ensure that substrate cleavage was complete and that the P RNA-3′ product complex was formed. Modification reactions were carried out using published protocols with minor modifications (12–14). Ten picomoles of P RNA in either the presence or absence of a substrate were modified with DMS or KE. The total reaction volume was 33 µl. The final concentration of tRNA, #4, #8 and #17 was >1 µM; that of #22 was 3 µM. These substrate concentrations are greater than four times the binding constant (~0.1 µM for #4 and #17, ~0.2 µM for #8 and ~0.8 µM for #22) as determined by non-denaturing gel electrophoresis. The final concentrations of DMS and KE were 105 mM (100-fold dilution from stock solution) and 15 mM (400-fold dilution), respectively. The reaction buffers were: (i) 30 mM HEPES, pH 7.9, 25 mM $MgCl_2$ for #4, #17 and #22; (ii) 30 mM HEPES, pH 7.9, 10 mM $MgCl_2$, 1 mM spermine for #8; (iii) 30 mM HEPES, pH 7.9, 100 mM $MgCl_2$, 0.6 M KCl for $tRNA^{Phe}$. Modification proceeded at 37°C for 5 min and was stopped by the addition of a 2.5-fold molar excess of β-mercaptoethanol over DMS or 2-fold molar excess of boric acid over KE. The mixtures were then ethanol precipitated using 3.3 µg *E.coli* tRNA as carrier. Pellets were resuspended in 150 µl of 50 mM K-acetate, 200 mM KCl, pH 7.0, and re-precipitated with ethanol three times. Samples were dried and resuspended in water prior to reverse transcription.

Reverse transcription of modified P RNA

Three DNA primers were used to visualize the modified P RNA. Primer 1 (5′-AAATGTAAGTGGTCTAACGTT CTGTAA) was complementary to nt 381–401; primer 2 (5′-AACCATCC CCTTGGAAGAATTGCC) was complementary to nt 256–279; and primer 3 (5′-CGACTGCCGTCCTTTTTTCGGATG) was complementary to nt 127–149 of *B.subtilis* P RNA. Modified P RNA (1.7 pmol) and 0.72 pmol ^{32}P-labeled primer in 3.5 µl were heated at 93°C for 1 min in 15 mM Tris–HCl, pH 7.5, 1.5 mM EDTA followed by quick cool on ice for 4 min. Reverse transcription was carried out in 50 mM Tris–HCl, pH 8.3, 8 mM $MgCl_2$, 30 mM NaCl, 1 mM DTT, 200 µM dNTPs and 0.9 U of AMV reverse transcriptase (United States Biochemical) in 5 µl at 50°C for 10 min. The reaction was stopped by the addition of 5 µl gel loading buffer (9 M urea, 50 mM EDTA, 0.01% each of xylene cyanol FF and bromophenol blue). Samples were boiled for 1 min and quick cooled on ice for 3 min prior to electrophoresis on 8% polyacrylamide gels containing 7 M urea. The gels were dried and visualized using a PhosphorImager (Fuji Medicals).

Figure 1. Primer extension of P RNA modified in the presence and absence of added substrates. Lanes U, G, A and C represent the RNA sequence derived from reverse transcriptase sequencing reactions of P RNA. The lane indicated by (–) represents a control for P RNA sequencing in which no dideoxy nucleotides were included. Lanes 'DMS' and 'KE' indicate the reagent used in chemical modification of P RNA. The substrate bound to P RNA during a particular P RNA modification reaction is indicated above the lane. Numbers followed by a dash indicate the nucleotide position in P RNA. Modified bases appear as reverse transcriptase stops one nucleotide position shorter than the actual modified nucleotide. An arrow indicates the particular nucleotide position in which protection was observed. (**A**) A130 (nt 172–115); (**B**) G180 (nt 183–141); (**C**) G220 (nt 224–218); (**D**) A230 (nt 248–223).

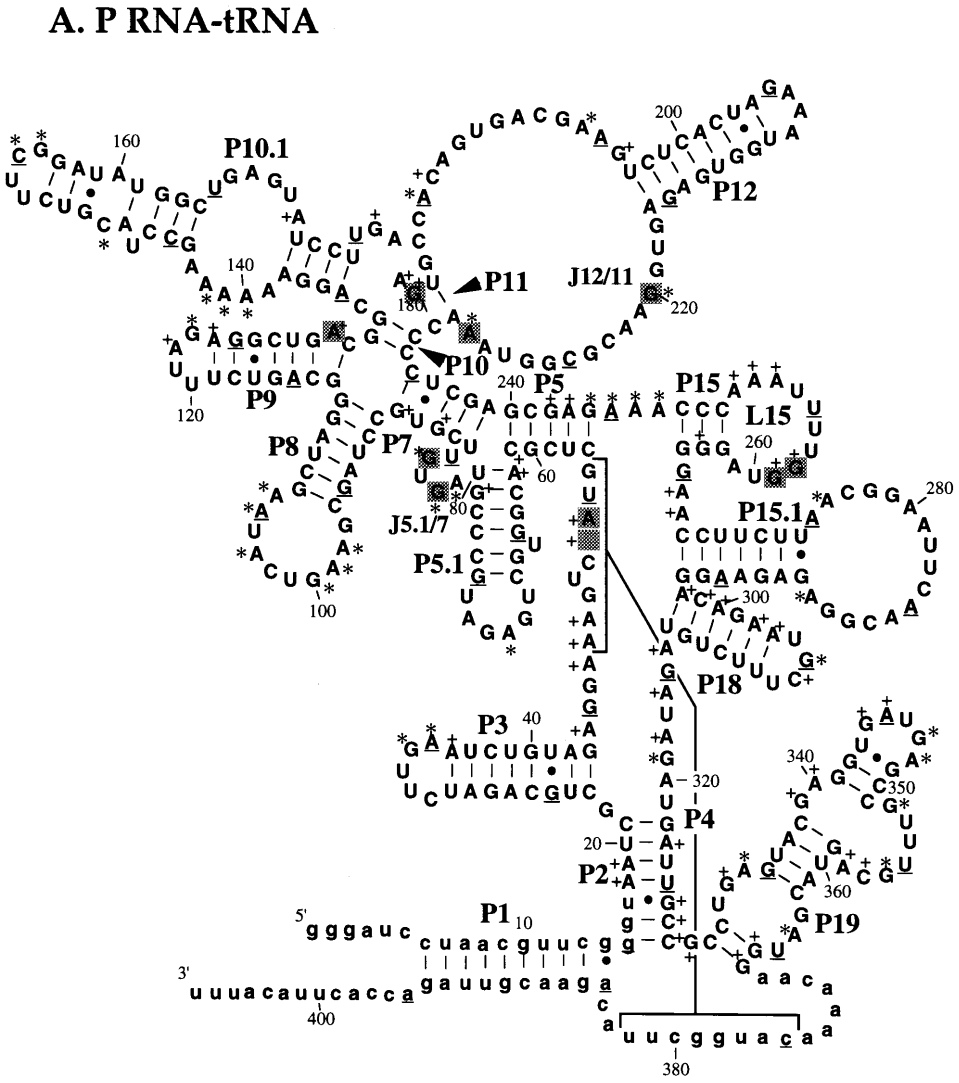

Kinetics of the selected substrates

All reactions were performed under single turn-over conditions with 10–1000-fold molar excess of P RNA over the 5′ ^{32}P-labeled substrate. The detailed procedure of single turnover kinetics has been described by Loria and Pan (5).

Structural mapping by nucleases

These procedures have been thoroughly described by Pan and Jakacka (8).

RESULTS AND DISCUSSION

Chemical modification of P RNA and P RNA-3′ product complexes

P RNA was chemically modified under three ionic conditions. Each condition was chosen to optimize binding between P RNA and each of its substrates. All three conditions contain Mg^{2+} concentrations significantly above that required for P RNA folding (9). Using three primers, ~85% of all nucleotide positions could be analyzed. Figures 1 and 2A summarize the *B.subtilis* P RNA modification pattern that resulted from DMS and KE modification at 37°C. Modifications are classified as strong or weak based on the intensity of the reverse transcriptase stops. Upon binding of the tRNA product, protection occurs at nucleotides A130, G180, G220 and A230 in the folding domain I of P RNA. This folding domain has been shown to directly interact with the T stem–loop of tRNA (4,5,15,16). Protection is also visible at nucleotides G258 and G259 in the CCA-3′ binding loop, L15 (17–19). Protection of nucleotides C53 and A54 in P4 can be attributed to P RNA interaction with the substrate residues around the cleavage site (3,4). The J5.1/7 region of *B.subtilis* P RNA is not conserved among bacterial P RNAs and protection of G82 and G84 in this region may be due to conformational changes that occur upon tRNA binding. Overall, our results agree well with those from Pace and co-workers (18) whose results were obtained under a different ionic condition and at lower temperature (50 mM HEPES, pH 7.8, 25 mM $CaCl_2$ and 1 M NH_4Cl, 0°C).

Chemical modification of P RNA reveals that binding of #4, #17 and #22 protects many of the same nucleotides as binding of

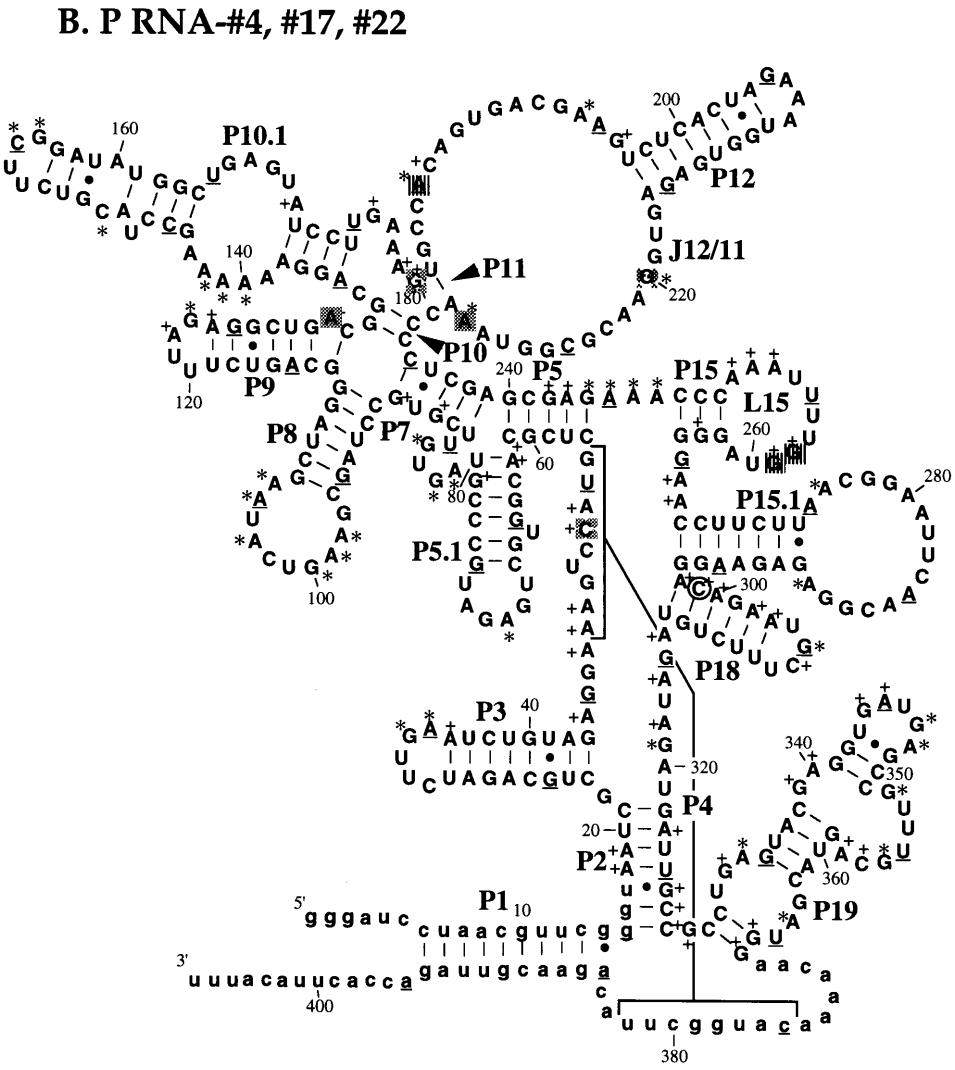

tRNA (Figs 1 and 2B). In particular, nucleotides that are known to interact with the T stem–loop in tRNA, A130 and A230, are protected by all three substrates. #4 and #17 also protect nucleotides G258 and G259 in loop L15, the binding site of the CCA-3′. #22 did not prevent modification of these nucleotides. This result agrees with the previous observation that the CCA-3′ of #22 has little effect on cleavage efficiency (7). Interestingly, protection of nucleotides G180, A185 and G220 differs for these three substrates. #17 binding protects all three residues; however, A185 is not protected by #22, and G180 and G220 are not protected by #4. These results suggest that the binding surfaces for these substrates overlap but are not identical.

Binding of #8 results in a unique protection pattern of P RNA (Figs 1 and 2C). Only three nucleotides are protected in the region known to bind tRNA. This result is consistent with the previous observation that little overlap exists between the binding site of #8 and that of tRNA (8). Interestingly, the deletion of nucleotides #62–239 does not affect binding of #8 to P RNA; however, this deletion has a large effect on the chemical step (8). It can therefore be assumed that protection of G82, G84 and G180 is induced by conformational change in P RNA rather than by substrate binding. Potential substrate binding site was identified using a P RNA construct containing nucleotides #240–401+#1–112 (10). This construct was modified while complexed with #8 and analyzed with a primer complementary to nucleotides #61–47 of P RNA. Extensive and strong protection is seen in the L1 region (Fig. 3C). This result provides physical evidence that #8 indeed interacts with the L1 region of P RNA.

Secondary structure and kinetic analysis of the selected substrates

The secondary structure of the selected substrates was probed with nucleases V1, T1 and S1 (Fig. 3). The nuclease mapping data is consistent with a secondary structure that contains a short helix around the cleavage site and a hairpin loop at the corresponding position of the T stem–loop in tRNA. These two helices are connected through a non-helical linker region that differs among these substrates.

The catalytic efficiency of the selected substrates is analyzed by single turnover kinetics (Table 1). Under these conditions, k_{cat} is pH dependent (data not shown) and may directly correlate with

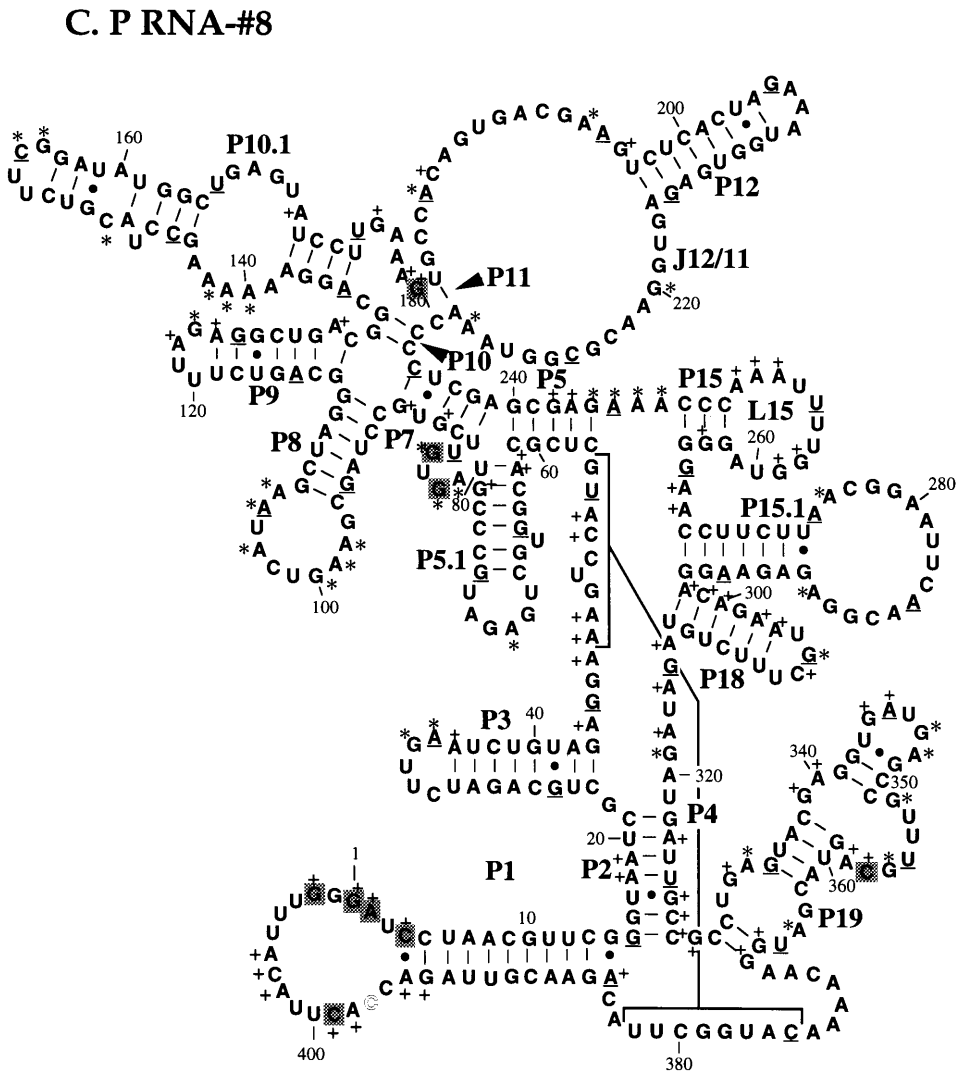

Figure 2. Summary of chemical modifications of P RNA. The positions of modified nucleotides in *B.subtilis* P RNA are imposed on its secondary structure. The modifications are designated as strong (✶) and weak (+) according to the relative accessibility of nucleotides to modification in P RNA. For the uncomplexed P RNA, the modification pattern was the same under all conditions tested here. Nucleotides protected upon substrate binding are generally shaded. Nucleotides represented by lower case letters could not be analyzed due to primer binding or gel resolution. (**A**) P RNA–tRNA complex. (**B**) P RNA–#4, #17 and #22 complex: stippled boxes indicate protection by all substrates; vertical striped boxes indicate protection by #4 and #17; diamond patterned boxes indicate protection by #17 and #22. The circled nucleotide C299 is only protected in the P RNA–#17 complex. (**C**) P RNA–#8 complex. The highlighted nucleotide C397 shows enhanced modification upon #8 binding.

the chemical step, k_2. Assuming that the k_{cat}/K_m approximates the on-rate for substrate binding, k_1, the K_m [= $(k_{-1} + k_2)/k_1$ under single turnover conditions] for #4 and #22 can be calculated to approximate K_d. However, it is likely that the dissociation rate, k_{-1}, of the tRNA and #17 substrates is comparable to k_2. The K_m for tRNA and #17 may, therefore, represent an overestimate of K_d. All selected substrates nevertheless appear to bind equally well or better than the tRNA substrate at 50 mM $MgCl_2$. The chemical step of the selected substrates, on the other hand, is significantly slower than that of a tRNA substrate. These results are consistent with the selection experiment in which binding is a far more dominant factor than the chemistry of the cleavage reaction (7). To test whether the protection observed in the chemical modification experiments faithfully detects direct ribozyme-substrate interaction, a P RNA double mutant of A185→G185/C186→U186 was tested kinetically (Table 1). Nucleotide A185 was protected by #4 and #17, but not by #22. Indeed, the K_m for #4 and #17 using the mutant P RNA increases by 36- and 8-fold compared to the K_m using the wild-type P RNA, whereas the K_m for #22 remains the same. K_m also increases by 8-fold for the tRNA substrate, suggesting that tRNA has another direct contact with P RNA that was not observed in the protection experiment. The protected nucleotides therefore only represent a fraction of all potential P RNA residues involved in substrate binding. The chemical step is not affected in the mutant, in agreement with our previous finding that disruption of a single interaction in the T stem–loop region has little effect on chemistry of the P RNA reaction (5). Since k_2 remains the same, the increased K_m for the mutant P RNA is likely to be due to faster k_{-1}. These K_m values therefore approximate K_d for all substrates.

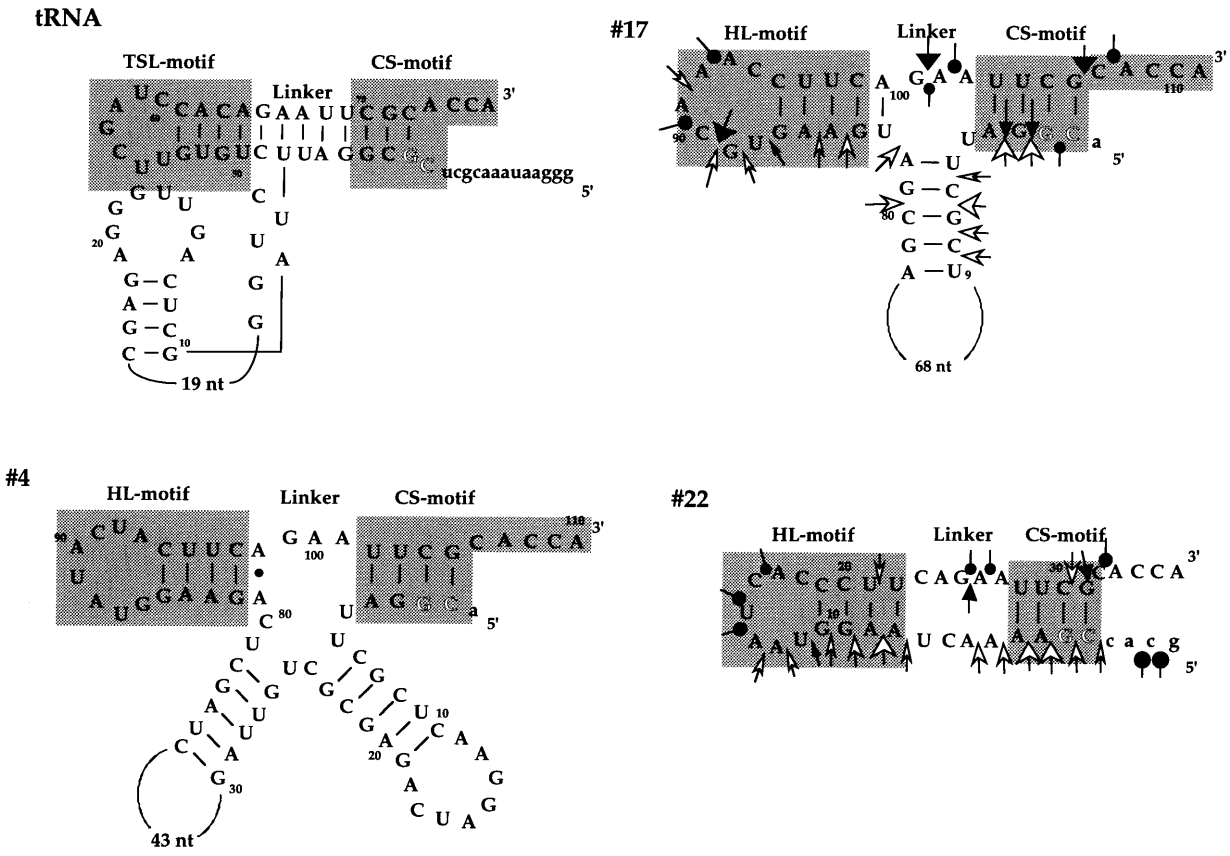

Figure 3. Proposed secondary structure of #4, #17 and #22 with cleavage site motif (CS) and the T stem–loop like motif (hairpin loop, or HL-motif) shaded. The tRNA^{Phe} substrate used in this work is also included for comparison. The linker regions in these selected substrates are non-helical, in contrast to a tRNA. The cleavage site is located between the two highlighted residues. Partial digestion by T1 (solid arrows), V1 (open arrows) and S1 (stem and solid circles) nucleases for #17 and #22 are indicated by arrows.

By this criteria, the G185U186 mutant affects binding of the tRNA and #17 substrates by >1.3 kcal/mol.

Table 1. P RNA cleavage of selected substrates under single turnover conditions

Substrate	K_m (μM)	ΔΔG (kcal/mol)[b]	k_2 (min^{-1})	ΔΔG (kcal/mol)[c]
P RNA (wild-type)[a]				
tRNA^{Phe}	0.24 ± 0.03	–	2.0 ± 0.1	–
#4	0.10 ± 0.03	–	0.30 ± 0.02	–
#17	0.046 ± 0.010	–	0.55 ± 0.02	–
#22	0.21 ± 0.05	–	0.08 ± 0.01	–
P RNA mutant (G185U186)[a]				
tRNA^{Phe}	2.0 ± 0.3	1.3	2.0 ± 0.3	0.0
#4	3.6 ± 0.4	2.2	0.36 ± 0.02	–0.1
#17	0.37 ± 0.10	1.3	0.71 ± 0.05	–0.2
#22	0.31 ± 0.08	0.3	0.039 ± 0.002	0.4

[a]Reaction conditions: 50 mM MES, pH 6.1, 50 mM $MgCl_2$, 0.2 M KCl (0 M for #22), 37°C.
[b]ΔΔG = –RT ln [K_m(w.t. P RNA)/K_m(mutant P RNA)].
[c]ΔΔG = –RT ln [k_2(mutant P RNA)/k_2(w.t. P RNA)].

Interaction of RNA structural modules

The coaxially stacked acceptor stem and T stem–loop in tRNA have been proposed to participate in P RNA binding as three distinct motifs: the cleavage site (CS) motif; the T stem–loop (TSL) motif; and a coaxially stacked linker region (Fig. 4; 8). The linker region in tRNA may be partially unstacked when tRNA is bound to P RNA (20,21). The secondary structure of the selected substrates, #4, #17 and #22, also contains the equivalents of the CS- and the TSL-motifs (Fig. 3). These two motifs are designated as structural modules in this work. The modules in a fourth selected substrate, #8, consist of a short helix around the cleavage site and a pseudoknot (8). The two modules in all selected substrates are connected through a non-helical linker region.

The two folding domains of P RNA can be thought of as two structural modules that bind substrate. Domain I of P RNA contacts the T stem–loop module of tRNA and, thus, confers substrate specificity. Domain II of P RNA directly contacts the acceptor stem/5′ leader module of tRNA. The two domains in P RNA bind the two modules in the selected substrates, #4, #17 and #22, in a similar fashion. Domain II of P RNA can additionally be broken down into two intradomain modules that bind substrate #8. One module contains the active site of P RNA and binds the cleavage-site module of #8. The other module contains the L1 region of P RNA and binds the pseudoknot module of #8 (Fig. 4).

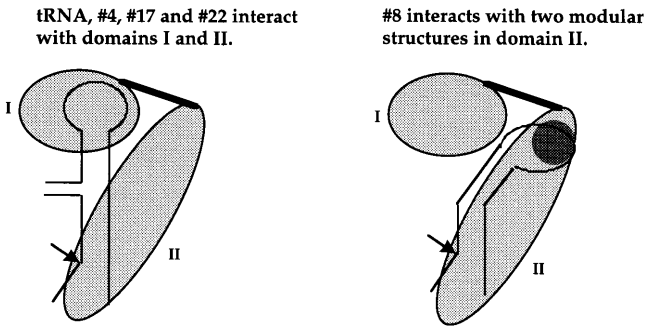

Figure 4. Interaction of structural modules in the P RNA–substrate complexes. The folding domains of P RNA are shown as light shaded ovals and the L1 region is shown as a dark shaded circle. The substrates are shown schematically with the cleavage site indicated by an arrow.

The binding properties of P RNA revealed by studies with our selected substrates can be exploited to isolate new ribozyme-substrate pairs by *in vitro* selection. Substitution of one module in the ribozyme (e.g. the T stem–loop binding domain or the L1 region) may be compensated for by substitution of another module (e.g. the hairpin-loop module or the pseudoknot module) in the RNA substrate.

ACKNOWLEDGEMENTS

This work was supported by a grant from NIH (GM52993) and a Junior Faculty Research Award from the American Chemical Society (JFRA-543) L.O. is a recipient of an undergraduate summer research fellowship from Howard Hughes Medical Institute and from the Richter Fund.

REFERENCES

1 Altman,S., Kirsebom,L. and Talbot,S. (1993) *FASEB J.*, **7**, 7–14.
2 Pace,N.R. and Brown,J.W. (1995) *J. Bacteriol.*, **177**, 1919–1928.
3 Westhof,E. and Altman,S. (1994) *Proc. Natl Acad. Sci. USA*, **91**, 5133–5137.
4 Harris,M.E., Nolan,J.M., Malhotra,A., Brown,J.W. and Pace,N.R. (1994) *EMBO J.*, **13**, 3953–3963.
5 Loria,A. and Pan,T. (1997) *Biochemistry*, **36**, 6317–6325.
6 Liu,F. and Altman,S. (1994) *Cell*, **77**, 1093–1100.
7 Pan,T. (1995) *Biochemistry*, **34**, 8458–8464.
8 Pan,T. and Jakacka,M. (1996) *EMBO J.*, **15**, 2249–2255.
9 Pan,T. (1995) *Biochemistry*, **34**, 902–909.
10 Loria,A. and Pan,T. (1996) *RNA*, **2**, 551–563.
11 Milligan,J.F., Groebe,D.R., Witherell,G.W. and Uhlenbeck,O.C. (1987) *Nucleic Acids Res.*, **15**, 8783–8798.
12 Moazed,D., Stern,S. and Noller,H.F. (1986) *J. Mol. Biol.*, **187**, 399–416.
13 Ehresmann,C., Baudin,F., Mougel,M., Romby,P., Ebel,J.P. and Ehresmann,B. (1987) *Nucleic Acids Res.*, **15**, 9109–9128.
14 Stern,S., Moazed,D. and Noller,H.F. (1988) *Methods Enzymol.*, **164**, 481–489.
15 Nolan,J.M., Burke,D.H. and Pace,N.R. (1993) *Science*, **261**, 762–765.
16 Pan,T., Loria,A. and Zhong,K. (1995) *Proc. Natl Acad. Sci. USA*, **92**, 12510–12514.
17 Kirsebom,L.A. and Svard,S.G. (1994) *EMBO J.*, **13**, 4870–4876.
18 LaGrandeur,T.E., Huttenhofer,A., Noller,H.F. and Pace,N.R. (1994) *EMBO J.*, **13**, 3945–3952.
19 Oh,B.-K. and Pace,N.R. (1994) *Nucleic Acids Res.*, **22**, 4087–4094.
20 Kahle,D., Wehmeyer,U. and Krupp,G. (1990) *EMBO J.*, **9**, 1929–1937.
21 Gaur,R.K., Hanne,A., Conrad,F., Kahle,D. and Krupp,G. (1996) *RNA*, **2**, 674–681.